Supporting Information

Piezocatalytic performance enhancement using the sandwich structure of PVDF–HFP/graphene film

Ya Liu, Wangshu Tong*, Wanting Song, Tingting Cao, Yulun Liu, Lingchao Wang, Zhihao Wang, Yihe Zhang*

Beijing Key Laboratory of Materials Utilization of Nonmetallic Minerals and Solid Wastes, National Laboratory of Mineral Materials, School of Materials Science and Technology, China University of Geosciences (Beijing), Beijing 100083, China

*Correspondence author. E-mail: tong@cugb.edu.cn; zyh@cugb.edu.cn.

Preparation of porous films: The rGO suspension drops were added to three glass slides (5×5 cm^2), wherein the volumes of titrated rGO solution were 0.05×2, 0.10×2, 0.15 mL $\times 2$, respectively. After rGO dried completely, 0.75 mL $\times 2$ PVDF–HFP solution was dropped into each rGO. The three weight percentages of 2.4, 4.7, and 6.9 wt% of rGO were obtained. When the rGO content exceeded 6.9 wt%, the excess rGO could not be loaded into PVDF–HFP.
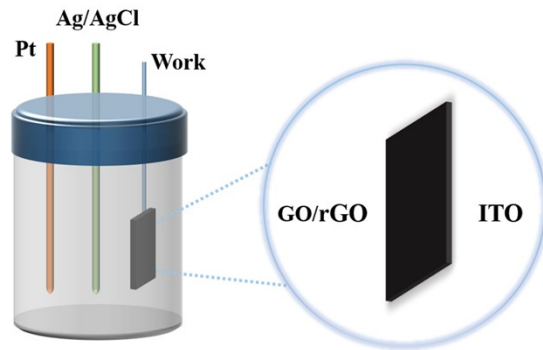
Figure S1. The schematic diagram of the electrochemical three-electrode system for GO and rGO.

Table S1. EIS fitting data for GO and rGO.

Types of electrode	R1/Ω	R2/Ω
GO	2.395	24.17
rGO	1.885	15.87

GO and rGO electrodes, inset shows equivalent circuit diagram. R1 is solution resistance; R2 is the total charge transfer resistance; Z is the impedance. The constant phase Angle element CPE1 is used instead of the ideal capacitor (**Figure 1c**).
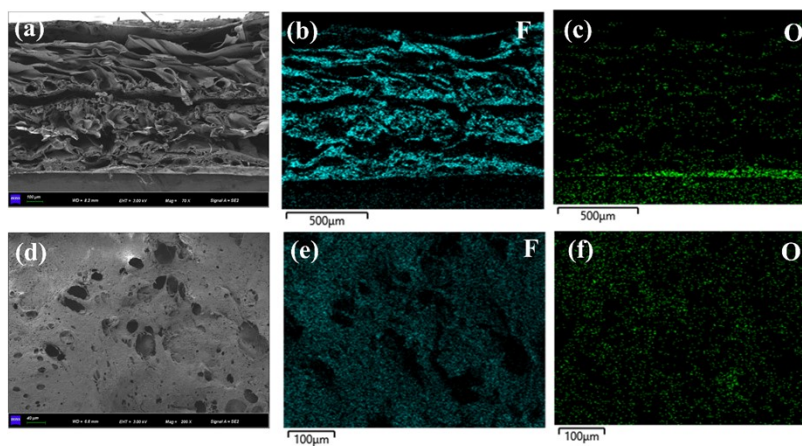
Figure S2. SEM and elemental color maps of (a−c) the PVDF–HFP@rGO porous sandwich film and (d-f) the PVDF–HFP/rGO porous composite film.

Equations S1.

(1) $$F(\beta) = A_\beta / (K_\beta / K_\alpha) A_\alpha + A_\beta$$

where A_β is the absorbance at 840 cm^{-1}, and A_α is the absorbance at 764 cm^{-1}. K_β (7.7×10^4 cm^2 mol^{-1}) and K_α (6.1x10^4 cm^2 mol^{-1}) are the absorption coefficients at 840 cm^{-1} and 764 cm^{-1}, respectively. The relative content of the β phase can be calculated from the equation above. The characteristic absorption peak of the β phase is about 840cm^{-1}.

(2) For X-ray diffraction, the Bragg's Law:

$$2d\sin\theta = n\lambda$$

Where d is the distance between the crystal planes, θ is the Angle between the incoming ray, the reflected ray and the reflected crystal plane, λ is the wavelength, n is the reflection order, Bragg equation is the necessary condition but not sufficient condition for X-ray diffraction in crystal.
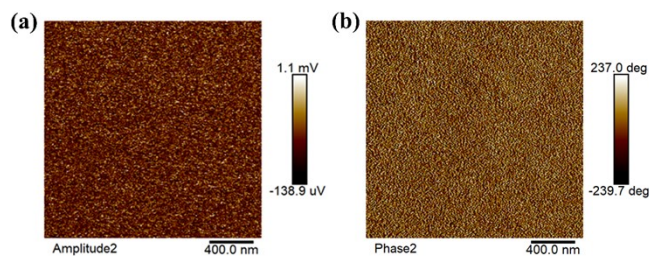
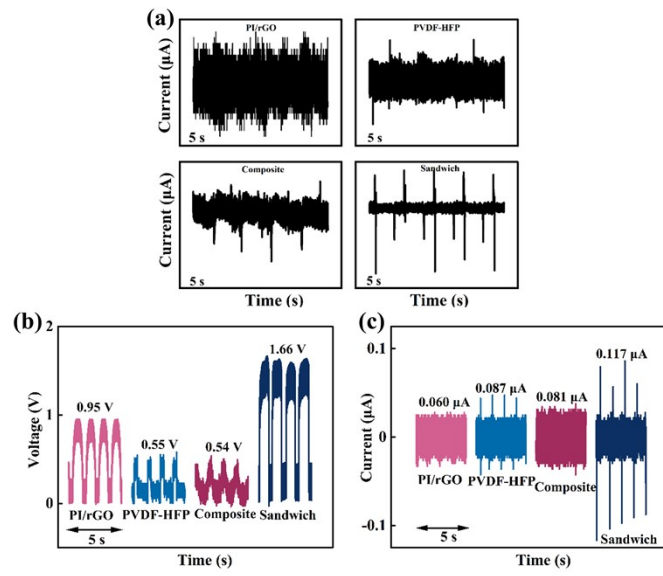**Figure S3.** KPFM image of PVDF–HFP@rGO film, (a) amplitude image; (b) phase image.

Figure S4. Piezoelectric signal (a) individual I_{SC} image. (b) V_{OC} and (c) I_{SC} with electrostatic shielding.
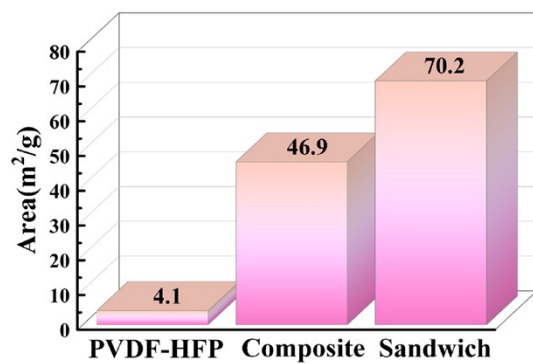
Figure S5. Comparison of the specific surface areas of PVDF–HFP, PVDF–HFP/rGO and PVDF–HFP@rGO samples.
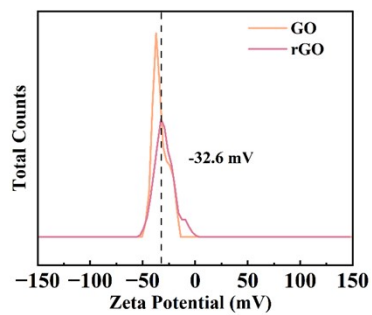
Figure S6. Zeta potential values of GO and rGO.

Table S2. Comparison of the degradation performances with different piezocatalysts.

| Piezocatalysts	Methods	Dye species	Dye volume and concentration	Degradation rate/%	Degradation time/h	Year Ref.
Fe$_2$O$_3$/PVDF–HFP	Magnetic stirring (300 rpm min^{-1})	TC	20 mL, 50 mg/L	53.7	11	2022 [1]
HPVDF/BTO–OVs	Propeller stirring (600 rpm min^{-1})	BPA	50 mL, 5 mg/L	33.0	1	2022 [2]
H–ZnS@SNG	Magnetic stirring (600 rpm min^{-1})	MB	20 mL, 20 mg/L	88.7	2	2021 [3]
PVDF–HFP@rGO	Magnetic stirring (600 rpm min^{-1})	MB	20 mL, 10 mg/L	98.0	1	This work
BaTiO$_3$	ultrasonic	MB	50 mL, 2 mg/L	91.3	2/3	2022 [4]
Ag@LiNbO$_3$/PVDF	ultrasonic	MB	10 mL, 5 mg/L	89.0	2	2021 [5]
SnS$_2$/CNFs	ultrasonic	BPA	10 mL, 10 mg/L	100.0	2	2021 [6]
OVHAP	ultrasonic	BPA	20 mL, 15 mg/L	85.6	1/2	2022 [7]
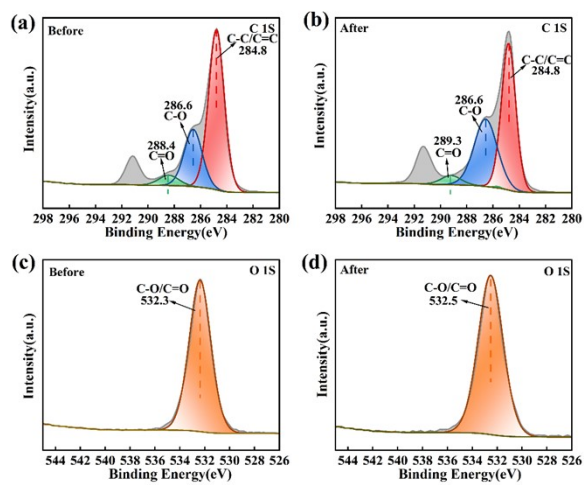
Figure S7. XPS survey spectrum of the PVDF–HFP@rGO: the change in the valence state before and after the reaction.
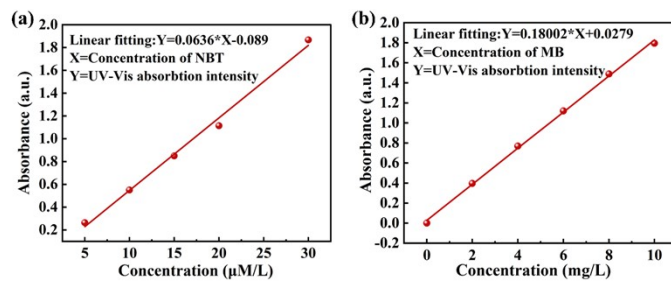
Figure S8. Standard curve of NBT and MB solution.

References:

1   M. Chai, W. Tong, Z. Wang, Z. Chen, Y. An and Y. Zhang, *J. Hazard. Mater.*, 2022, **430**, 128446.

2   L. Wan, W. Tian, N. Li, D. Chen, Q. Xu, H. Li, J. He and J. Lu, *Nano Energy*, 2022, **94**, 106930.

3   M. Pan, S. Liu, B. Pan and J. W. Chew, *Nano Energy*, 2021, **88**, 106312.

4   Q. Tang, J. Wu, D. Kim, C. Franco, A. Terzopoulou, A. Veciana, J. Puigmartí-Luis, X. Z. Chen, B. J. Nelson and S. Pané, *Adv. Funct. Mater.*, , DOI:10.1002/adfm.202202180.

5   G. Singh, M. Sharma and R. Vaish, *ACS Appl. Mater. Interfaces*, 2021, **13**, 22914–22925.

6   W. Tian, J. Qiu, N. Li, D. Chen, Q. Xu, H. Li, J. He and J. Lu, *Nano Energy*, 2021, **86**, 106036.

7   Y. Miao, W. Tian, J. Han, N. Li, D. Chen, Q. Xu and J. Lu, *Nano Energy*, 2022, **100**, 107473.